Journal of Electroceramics 3:4, 329–346, 1999

FEATURE ARTICLE

Conducting Polymer Composites

R. STRÜMPLER & J. GLATZ-REICHENBACH
ABB Corporate Research Ltd., CH-5405 Baden-Dättwil, Switzerland

Submitted January 8, 1999; Revised April 1, 1999; Accepted April 14, 1999

Abstract. Conducting polymer composites become increasingly important for technical applications. In this article, the resulting electrical properties of such materials are illustrated by a variety of experimental examples. It is shown that the combined mechanical, thermal and electrical interaction between the filler particles via their electrical contacts and the surrounding polymer host matrix are responsible for the properties of the composite material. A short review is given of the theoretical background for the understanding of the electrical transport in such materials. The arrangement of the filler particles and the resulting conductivity can be described either by percolation or by effective medium theories. It can also be related to different types of charge carrier transport processes depending on the internal composite structure. Special emphasis is given to the microstructure of the filler particles such as size, hardness, shape and their electrical and thermal conductivities. A detailed analysis of the physics of the contact spots and the temperature development during current flow at the contact is given. It is shown that the polymer matrix has a strong influence on the electrical conductivity due to its elastic properties and the response to external thermal and mechanical stimulation. Strong changes in the electrical conductivity of conducting polymer composites can be realized either by thermal stimuli, leading to a positive and negative temperature coefficient in resistivity, or by applying mechanical stress. By using nonlinear fillers an additional degree of functionality can be achieved with conducting polymers.

Keywords: polymer composites, electrical conductivity, filler properties, nonlinearity

1. Introduction

When an electrically conducting phase is dispersed in sufficient quantity in a polymeric resin, a conductive composite is formed. The unique properties of such composites make them technologically superior to or more cost effective than alternative materials. Since the first experimental results were published decades ago, conducting polymer composites have been adapted to a variety of applications.

The primary applications for conductive composites involve electromagnetic interference (EMI) shielding. EMI shielded enclosures are mainly designed to protect against radiation. The largest market in this area is housing for business machines. In addition, conductive composites can be used to shield individual electronic components, which are either particularly noisy or particularly sensitive to outside electromagnetic noise. In the EMI shielding market, conductive composites compete with a number of other technologies based on surface coating. These methods include vacuum metallizing, sputter coating, zinc arc spraying, nickel-based paints, and electroless metal coatings.

A related and less demanding application is for electrostatic dissipation (ESD), to bleed off charge continuously as a means of preventing harmful arcing discharges. The requirements for ESD are similar to those of EMI, but the level of conductivity required is lower: resistivities of 10^2–$10^6\,\Omega\,\mathrm{cm}$ are adequate to bleed off electric charges rapidly. Applications include chip and circuit board carriers for shipping of electronic equipment. Antistatic protection is also required for parts in conveyor belts, weaving machine

arms or airplane tires, where relative motion between dissimilar materials occurs [1].

Direct platable plastics are conductive composites that are electrically conductive enough to be electroplated directly without a metal coating. As a result, prior metallization or other surface conductivity treatments are unnecessary, leading to cost savings. For direct plating to occur, the plastic itself must be able to carry the current only during the initial stages of metal deposition. Once plating has been initiated and the covering of the plastic surface is complete, the growing electrodeposited metal layer becomes the primary current carrier. While a resistivity of less than $10\,\Omega\,\mathrm{cm}$ is desirable, materials with up to $1000\,\Omega\,\mathrm{cm}$ can be plated [2]. Potential applications are metal-plated automotive parts for both interior and exterior use [3] or as small decorative parts such as cosmetic packages, bottle caps or toys.

In electronic applications, conductive filled polymers are useful as adhesives and circuit elements. These materials normally consist of silver powder incorporated in a variety of polymers, including epoxy, silicone, polyurethane, and polyimide. Their utility arises from their very low electrical resistivities (in the order of $1 \times 10^{-4}\,\Omega\,\mathrm{cm}$) and high thermal conductivities ($\approx 1\,\mathrm{W/mK}$). The positive temperature coefficient of resistance (PTCR) of conductive composites [4] is used for self-limited heating systems and fault current limiters in circuit protection. The later devices consist commonly of carbon black in a matrix of polyethylene. When the composite is heated by the passage of electrical current, the volume expansion near the melting point of the semi-crystalline polymer disrupts the conductive filler network, causing the resistance of the composite to increase tremendously. The composite thus shows two distinct, current-dependent behaviors. At low current, it conducts electricity efficiently, but it becomes a current limiting device when it is heated by a sufficiently high current. Commercial devices are available for electronic circuit protection [5]. Examples are protection against short circuit faults by external devices in computers [6] or protection of batteries against short circuit discharge [7,8]. For low voltage distribution systems, current limiters are available up to ratings of 63 A [9].

For the commercial use of conducting composites, a complete understanding of their properties is necessary. Considerable effort has been devoted over several decades to experimental studies of the electrical resistivity of polymer composites [10–12]. In order to study the effect of filler on the dynamic electrical and mechanical properties of the polymer matrix, dielectric spectroscopy has been applied extensively [13,14]. As an example, dielectric measurements have been used to characterize composites with different types of carbon black, and with variable degrees of dispersion and loading levels [15]. It has also been shown that interfacial polarization, i.e., the well known Maxwell-Sillar-Wagner Effect, plays an important role in the electrical relaxation and a.c. conductivity of composite materials at frequencies up to the GHz range [16]. Also a number of attempts have been made to provide a theoretical description of the conduction mechanisms [17–22]. A good understanding of current conduction between the grains embedded in the polymer, in contact as well as separated, and heat generation and conduction within the grains and matrix, is imperative in understanding the material and the limitations of devices built from it. Despite of all the work, which has been done, a complete understanding of these materials is still lacking. In this paper we try to give an overview of the experimental and theoretical background.

2. Conduction Mechanism

Polymer composites consist of at least two components, a polymer matrix and a filler. The filler can be an inorganic powder such as a metal or a ceramic, or an organic material such as carbon (carbon black or a fullerene) or an intrinsically conducting polymer. The conductivity depends critically on the volume content of the filler. For very low filler fractions, the mean distance between conducting particles is large and the conductance is limited by the polymer matrix, which has typically a conductivity in the order of $10^{-15}\,\Omega^{-1}\,\mathrm{cm}^{-1}$ (Fig. 1). When a sufficient amount of filler is loaded, the filler particles get closer and form linkages, which result in an initial conducting path through the whole material. The corresponding filler content is called the percolation threshold. In this concentration range, the conductivity can change drastically by several orders of magnitude for small variations of the filler content. Finally, at high loading of the filler, the increasing number of conducting paths forms a three-dimensional network. In this range the conductivity is high and less sensitive to small changes in volume fraction. In order to create a well conducting polymer

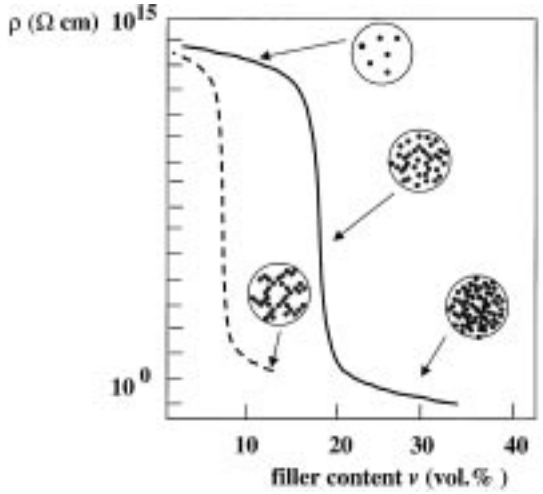

Fig. 1. Schematic sketch of the resistivity of a composite as a function of filler concentration for isotropic particles (full line) and carbon black (dashed line).

composite, the filler's conductivity has to be much higher than the matrix. It can vary from $10^5\,\Omega^{-1}\,cm^{-1}$ for metals like Ni, Ag or TiB_2 to intermediate conducting materials like carbon black around $0.1–10\,\Omega^{-1}\,cm^{-1}$ and low conductive fillers such as doped ZnO or SiC with low-field conductivities around $10^{-10}\,\Omega^{-1}\,cm^{-1}$.

2.1. *Connectivity*

The concept of connectivity was introduced by Newnham et al., in 1978 in order to classify different types of bi- or multiphase materials [22,23]. Each phase in a composite may be self-connected in zero, one, two, or three dimensions. The connectivity of a two component composite system is described by a two digit combination (i.e., *a*-*b*) with values for *a* and *b* between 0 and 3, respectively, describing the dimension of connectivity of each sub-phase.

For composites with very low content of isotropic filler particles, i.e., when each conducting particle is insulated by the surrounding matrix, the connectivity is 0–3. For dense packing of the filler in the matrix, when the filler particles form a three-dimensional network, the connectivity is 3–3. A transition from the insulating to the conducting state via thermal or mechanical dimensional changes can be understood as a change in connectivity from 0–3 to $x-3$ with $x > 0$. Accordingly, parallel fibers well distributed in a matrix have connectivity 1–3, and parallel conducting sheets have connectivity 2–3.

2.2. *Percolation Theory*

Percolation theory gives a phenomenological description of the conductivity of a system near to a metal-insulator transition. Excellent introductions are given by Zallen [24] and Staufer [25]. In model percolation studies one starts with a large, preferably infinite regular periodic lattice. A site of this lattice is then assigned at random with a probability *P*. All sites are bonded to adjacent sites by a conductive bond. At a critical probability P_c an infinite conducting cluster is first formed in the infinite lattice. This means that at an initial percolating path through the material the conductivity σ of the lattice changes from insulating to a finite value. Above P_c the conductivity is found to increase as

$$\sigma(P) \propto (P - P_c)^n \tag{1}$$

with a parameter n between 1.65 and 2 for three-dimensional lattices [21,23,26,27]. P_c is called the critical or percolation threshold.

Percolation theory is often limited to the cases in which either the insulating medium has zero conductance or the conducting filler has zero resistance. For real systems, where the resistivities are always finite values, percolation theory becomes valid with the use of scaling factors [28]. Critical volume fractions v_c have to be calculated by using filling factors [16]. For random packing in three dimensions v_c turns out to be about 16%.

The percolation behavior can be influenced by the shape of the filler. Fibers show, for example, a percolation threshold of only several percent. Additionally, geometry and dimension of the regarded composite sample, as for example, the distance of external electrodes have to be considered. Monte Carlo simulations and measurements on the same system of Ag-powder filled silicone rubber demonstrate the shift of percolation threshold to higher values with a decreasing ratio of electrode distance to filler particle size [29].

2.3. *Effective Media Theories*

In an effective media theory of a composite, a spherical or ellipsoidal grain is considered to be

surrounded by a mixture, which has the effective conductivity of the composite medium. It is mainly applied to composite systems with well separated subphases for the prediction and explanation of large-volume average values of electrical, thermal and diffusion properties. An excellent overview has been given by Landauer [30].

There are two special cases for which effective media theories exist, called the symmetric and the asymmetric cases. The symmetric case assumes that all space is filled by a random mixture of spherical (or ellipsoidal) particles of two or more components. When one component is a perfect insulator, the symmetric media theory contains a conductor-insulator transition. In the asymmetric case, the surface of the particles of one component is always completely covered by the other component. This means either a 0–3 or 3–0 connectivity. This case does not contain a transition. In order to describe the conductivity of conductor-insulator composites, McLachlan proposed a generalized effective media (GEM) equation [31,32]. It is derived as an interpolation between the symmetric and asymmetric effective media theories and has the mathematical form of a percolation equation within the appropriate limits. The GEM has been successfully applied to describe the piezoresistive behavior of Fe_3O_4 filled flexible epoxy [22]. A change in the resistivity of five orders of magnitude, from 10^{10} to $10^5\,\Omega\,\mathrm{cm}$, could be described by the GEM equation in good agreement with the experimental data.

2.4. Charge Carrier Transport in Composites

The process of charge carrier transport can be divided into two steps, the injection of charge carriers into the material (e.g., Fowler-Nordheim or Richardson-Schottky transmission types) and the motion of charge carriers through the material via hopping, tunneling, ballistic transport, diffusion, or metallic conduction. Extended reviews of charge carrier injection and transport in insulators as well as conductors have been presented elsewhere [33,34].

In diphasic composites four different conduction aspects have to be taken into account: the conduction in the polymer matrix, in the filler material, between adjacent filler particles and from the filler into the matrix and vice versa. Three different regimes of charge carrier transport are possible, which are governed by the morphology of the compounded material [18].

(i) For composites with very low filler loading well below the percolation threshold, it is expected that the mean distance between conducting filler-particles is large and no conducting paths throughout the whole composite are established. The mean separation distance of next neighbor filler particles d is larger than 10 nm, which means that even tunneling from particle to particle cannot take place. In this case, the composite conductivity is the result of transport processes within the polymer host matrix. Therefore, the loading has at low fields little effect on the electrical conductivity of the entire composite (Fig. 1).

(ii) In the second case, the filler-particles are still well separated, but their mean distance is below a certain threshold mean particle-particle distance of $d = 10\,\mathrm{nm}$. In this case electrical field assisted tunneling can occur between neighboring filler-particles as suggested by Beek [35].

The following equation gives an expression of the electrical field dependence of the tunneling current.

$$j_{\mathrm{Tunneling}} = A \cdot E^n \cdot \exp\left(-\frac{B}{E}\right) \tag{2}$$

The factor $\exp(-\mathrm{B/E})$ characterizes the transition probability of charge carriers from the filler into the polymer and vice versa. The value B is a measure of the energy barrier between the polymer and the filler material.

Alternatively, a model introduced by Frenkel [36] suggests an electrical field assisted hopping mechanism (i.e., electron-hole separation) for the charge carrier transport according to:

$$j_{\mathrm{hopping}} = A_R \cdot T^2 \cdot \exp\left(\frac{K \cdot E^{1/2}\Phi}{k_B \cdot T}\right) \tag{3}$$

This equation has been successfully applied, for example, to describe the charge carrier transport in mono-component toner material, i.e., carbon black (CB) filled polymer [37]. In this context, both the polymer matrix and the CB particles determine the charge carrier transport through the composite. The surface properties of the filler particles, the interfacial region, and the work function of both materials are important.

In Eq. 2 and Eq. 3, $A_R = 1.2\,10^6\,\mathrm{A/K^2\,m^2}$ is the Schottky-Richardson constant. A, B, n (with typical values between 1 and 3) and K are constants, Φ is the work function of the filler material, k_B the Boltzmann constant, T the temperature, and E is the applied

electric field strength. For composite systems close to the percolation limit, the conductivity is thus determined by the properties of the polymer, the filler material, the interface and, of course, by the dispersion of the filler material in the polymer.

(iii) Finally, at sufficiently high loading the conducting filler particles are in close contact, touching each other. The conduction of charge carriers occurs through the continuous structure of the chain of filler particles in the polymer matrix. The conductivity is mainly determined by the filler material and its microscopic contacts to adjacent filler particles.

2.5. *Electrical Contacts Between Filler Particles*

The resistance of the contact spots is the leading contribution to the overall composite resistivity, particularly for good conducting filler materials [38]. Two effects contribute to the contact resistance, the *constriction resistance* (Fig. 2a) of a contact spot and the *tunneling resistance* between the particles according to Eq. 2 [39]. Therefore the contact spots are the region of largest resistance and thus of highest electrical losses and may be the source of large temperature development during current flow through the composite.

If for the calculation of the constriction resistance hard spheres are assumed, with a Young's Modulus going to infinity, the spheres show contact to each other at only one point. This results in singularities of the contact resistance and the current density, without

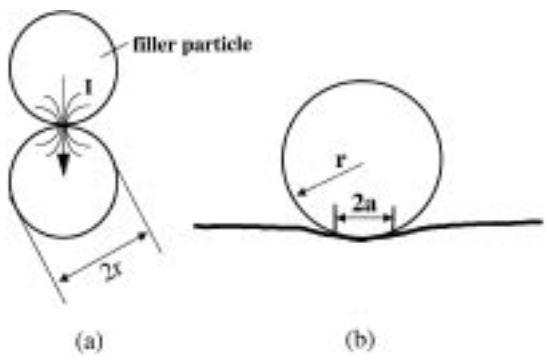

Fig. 2. (a) Sketch of two adjacent filler particles. The current through the grains is constricted at the contact point. (b) A protrusion of one filler particle in contact with a flat surface of another. The contact spot radius is a and the protrusion radius at the contact point is assumed to be equal to the particle radius r.

any dependence on an applied external force. In order to avoid these singularities and in agreement to macroscopic contacts, a contact spot with a finite radius, as shown in Fig. 2b, was first introduced by Holm [38].

The constriction resistance R_c at a circular contact area with radius a is given by Eq. 4 as already well known from the study of macroscopic electrical contacts [38]:

$$R_c = \frac{\rho_T}{2a} \tag{4}$$

Here, ρ_T is the bulk resistivity of the filler particles. The constriction resistance at the contact spots dominates over the bulk resistance of the filler particle as long as the contact spot radius a is much smaller than the filler particle radius.

Let us consider TiB_2 as a model filler material, since it is hard and rather resistant to oxidation. Assuming a bulk resistivity of $\rho_T = 1.5\,10^{-5}\,\Omega\,\mathrm{cm}$ and a contact spot radius of $a = 75\,\mathrm{nm}$, we calculate a contact resistance of $R_c = 1\,\Omega$. The particles are assumed to be spherical, all having the same size and being arranged on a cubic lattice. If the inter-particle resistance R_c is constant for all contacts, the specific resistivity can be derived from

$$\rho = R_c \times \frac{N_\parallel}{N_\perp} \tag{5}$$

where $N_\parallel$ is the particle density parallel to the direction of the measuring current and $N_\perp$ is the particle density perpendicular to the current flow. For particles with $r \approx 100\,\mu\mathrm{m}$, we get $N_\perp = 10^4\,\mathrm{cm}^{-1}$ and $N_\parallel = 100\,\mathrm{cm}^{-1}$, which results in a resistivity of $0.01\,\Omega\,\mathrm{cm}$. This is in good agreement with experimental results ($8.2\,10^{-3}\,\Omega\,\mathrm{cm}$) as listed in Table 1.

Equation 4 is valid only for filler particles of homogenous resistivity, negligible surface contamination, weak temperature dependent resistivity, and excluding large temperature gradients under current flow.

For filler materials with a surface oxide layer or other forms of surface contamination, the additional resistance contribution has to be added to R_c to obtain the correct contact resistance. For other than circular contact spot shapes a general expression can be found elsewhere [38].

2.5.1. The contact spot area. For a more realistic description of the contact resistance and an estimation

Table 1. Specific resistivities of Ag powder in silicone rubber [49] and TiB_2 in Spurr epoxy

Polymer	Filler	Filler content (vol. %)	Specific resistivity ($10^{-3}\,\Omega\,cm$)
Rubber	Ag 0.5 μm	15	12.0
	Ag 1.0 μm	15	2.90
	Ag 0.5 μm	20	7.10
	Ag 1.0 μm	20	0.49
Spurr epoxy	TiB_2, 45–63 μm	35	44
	TiB_2, 63–100 μm	35	37
	TiB_2, 100–200 μm	35	8.2

of the contact spot area, the mechanical properties of the filler material have to be taken into account. The radius a of the contact spot can be calculated from the elastic properties of the filler particles if the force between them and the particle radius r is known.

We assume that the contact arises between a protrusion or sharp edge of one particle and a flat surface of a neighbor particle (Fig. 2b). If the protrusion has the radius r at the contact spot, the elastic force F between the grains is for small deformations given by [40]:

$$F = \frac{2}{3}\frac{E}{1-\nu^2}\frac{a^3}{r} \tag{6}$$

where E is Young's modulus and ν the Poisson's ratio. Solving Eq. 6 for the parameter a and inserting it into Eq. 4 yields the constriction resistance:

$$R_c = \frac{1}{2}\rho_T\left(\frac{2}{3}\frac{E}{1-\nu^2}\right)^{\frac{1}{3}}F^{-\frac{1}{3}}r^{-\frac{1}{3}} \tag{7}$$

From this formula we learn that a decreasing contact resistance can be expected for increasing force F and increasing protrusion radius r. In practice r is difficult to determine. It may depend on the particle radius itself, but strongly depends on the plastic deformation of the particle. The easier the particle can be deformed under applied force, the larger the protrusion radius becomes. Hence, soft filler materials can be expected to yield smaller constriction resistance compared to hard materials.

The numerical prediction of the contact forces between filler particles in a composite is a very difficult problem because of the irregular shape and distribution of the filler. In order to overcome this problem a way of computing the average force from thermal expansion data using a thermoelastic mean-field model can be applied. When a large difference of the thermal expansion coefficients α between the composite and the pure matrix material is observed, the filler particles form a rigid skeleton within the matrix with consequently large contact forces. For smaller differences on the other hand, the structure is less rigid, with smaller forces. This is an indirect approach and requires exact thermal expansion data for the materials under consideration. The basic idea has also been used to derive relations between thermal expansion and bulk modulus for composites [41,42]. A direct approach, i.e., to calculate forces directly from first principles, seems exceedingly difficult since forces strongly depend on filler properties, morphology, and cluster structure. For low filler contents there are several attempts described in the literature [43,44], but they do not work well at high filler fractions.

2.5.2. The contact spot temperature. One important question to ask is: What is the temperature developed at the contact spots during current flow? The contact spots between filler particles may be subject to severe heating because of the constriction resistance and the resulting large current and power densities (see Fig. 2a for illustration).

By comparing the equations for thermal and electrical conduction within the filler particles, one can give a simple relation between the temperature T_{cs} of the contact spot and the voltage drop U across the contact [38]:

$$\int_{T_0}^{T_{cs}} \rho(T)\cdot\lambda(T)dT = \frac{U^2}{8} \tag{8}$$

where T_0 is the grain temperature far away from the contact region, and $\lambda(T)$ and $\rho(T)$ are the thermal conductivity and the electrical resistivity of the grain material, respectively. This relation is a quite remarkable one as the voltage across a contact turns out to be independent of the current and any

geometrical detail of the contact spot region, e.g., the contact cross section. This simplicity originates from the similarity between the equations for electrical current and thermal transport and from the fact that for this system equipotential and isothermal surfaces coincide.

Most good conductors satisfy the Wiedemann-Franz law,

$$\rho(T)\lambda(T) = LT \tag{9}$$

(L = Lorenz number $= 2.4 \cdot 10^{-8}\,(\mathrm{V/K})^2$ [45]), which basically states that good electrical and good thermal conduction go hand in hand. For materials which obey the Wiedemann-Franz law the integration in Eq. 8 can be performed and T_{cs} becomes:

$$T_{cs} = T_0\sqrt{1 + (U/U_0)^2} \tag{10}$$

with $U_0 = 2T_0\sqrt{L}$. For a grain temperature $T_0 = 300\,\mathrm{K}$, we obtain $U_0 = 0.093\,\mathrm{V}$. In Fig. 3 the contact spot temperature T_{cs} is plotted as a function of the voltage drop U across the contact for three different ambient temperatures T_0. The temperature inside the grain far from the spot (denoted as ambient) is seen to have hardly any influence at all on the temperature of the contact spot.

Extended scanning probe microscopy (SPM) and atomic force microscopy (AFM) studies on TiB_2 particle-particle contacts by Heuberger et al. [46] showed that in 1-V characteristics a strong non-linearity occurs around 0.1–0.5 V. For rising voltage the conductivity increases more and more until the voltage is limited to about 1 V. According to Fig. 3, the contact temperature should be about 1400°C at 0.5 V. Probably the hot contact spot at this temperature is already enlarged due to plastic flow of the filler material, which means a reduction of the contact resistance. This effect is also seen on metallic contacts at a lower voltage level [47]. The limitation to 1 V is caused by melting of the contact spots. As shown in Fig. 3, theory predicts that the melting temperature of TiB_2, $T_m = 2900°\mathrm{C}$, is reached at a voltage $U = U_c = 0.98\,\mathrm{V}$. If the contact region melts, its cross section and therefore its conductance increases dramatically. As a consequence, U_c is the maximum voltage sustained by the contact. The value of U_c is in excellent agreement with the experiments of Heuberger et al. [46].

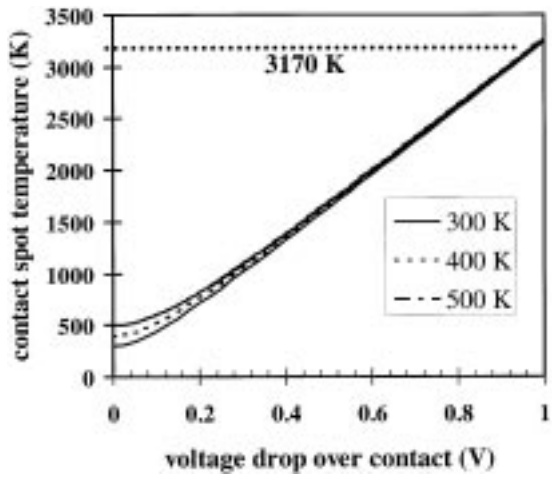

Fig. 3. Temperature at the contact spot according to Eq. 10 plotted as a function of the voltage drop over the contact for three different ambient temperatures.

3. Influence of the Filler on the Conductivity

The conductivity models described in section 2 are based on more or less idealized and simplified materials. In practice, the materials, which are available and used for conducting composites, exhibit special properties or morphologies, which have a severe influence on the overall conduction mechanism. In this section, we will consider the influence of several filler properties.

3.1. Filler Size

As indicated by Eq. 7, the constriction resistance decreases with increasing particle radius. If the protrusions which form the contacts are assumed to be larger in radius with increasing particle size, larger filler particles should result in a lower composite resistivity. This is supported by experimental data. Figure 4 shows the specific resistivity of TiB_2 filled high-density polyethylene for different particle size distributions. The filler content is 55 vol. % for 1–5 μm particles and 50% for all other sizes. TiB_2 is a good conducting material with reported conductivities between 9 and 35 $\mu\Omega\,\mathrm{cm}$ [48]. The graph shows that the resistivity decreases for increasing particle size. The strongest effect is observed between 1–5 μm and 10–30 μm. In this range the resistivity changes by about one order of magnitude. If 50 vol. % is occupied by the 1–5 μm particles, the difference would be even

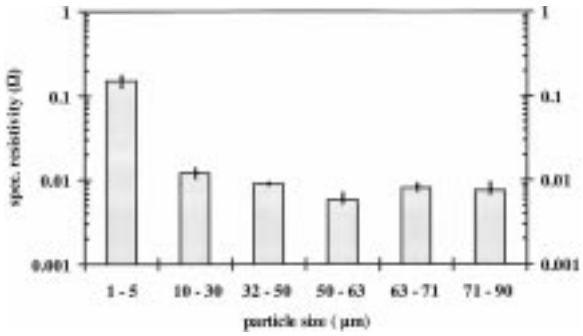

Fig. 4. Specific resistivity of HDPE/TiB_2 for different particle size distributions. The filler content for 1–5 μm particles is 55 vol. %, for all others it is 50 vol. %.

larger. The same trend is observed for 35 vol. % TiB_2 in Spurr B epoxy, as shown in Table 1. Particles of 100–200 μm have a four times smaller resistivity than 50 μm particles. The same trend has been reported by Ruschau et al. [49] for fine silver powder in a silicone rubber (Table 1). Again, the resistivity decreases for increasing particle size.

The filler size also has a strong influence on the heating of a composite by an electrical current. A reduction of the particle size leads to a larger number of contacts and smaller volumes of polymer matrix material embedded within the network of metallic filler particles. Due to a reduced mean distance of the matrix material to the next neighboring particle contacts, where the energy is generated, the heating of a composite with smaller filler particles should occur faster [50]. Together with the properties of the polymer matrix this is important for nonlinear changes of the resistivity on temperature increase. We will come back to this topic in section 4.4.

Nanometer-sized particles of metals and semiconductors have been investigated intensively in recent years because of the influence which their dimensions have on their electronic properties. It has been shown, for example, that metallic nanowires exhibit periodic quantization steps in the conductance [51]. Polymer composites containing metallic nanoparticles have been prepared by different means [52,53]. An overview of various ac and dc measurements has been given by Van Staveren et al. [54]. Applications are expected in microelectronics using in particular the single electron tunneling effect [55], although a lot of research is still necessary.

3.2. Filler Hardness

The contact resistance depends on the physical properties of the filler and its surface. As shown by Eq. 7, the constriction resistance increases for increasing Young's modulus. This means the softer the filler material, the larger is the contact spot area due to deformation. Hard fillers such as ceramic silicides, borides or carbides, lead to small point-like contact spot areas. If no surface oxide layers are formed, even these small contacts can provide relatively high conductivities. TiB_2, for example, is known to be rather resistant to oxidation. In an oxygen atmosphere only a thin layer of boron oxide (i.e., B_2O_3) is formed [56]. Boron oxide is rather soft and has, compared to TiB_2, a relative low melting point of about $T = 1200°C$ [57]. It can be expected that this thin oxide layer may be perforated already at fairly low contact pressure. And indeed, epoxies and thermoplastics filled with 50 vol. % TiB_2 particles show room temperature resistivities of only a few $10^{-3}\,\Omega$cm [58]. One main advantage of hard particles is that they do not stick together. Hence, the contact is easy to release by reducing the contact pressure [59].

On the other hand particles of ductile metals, e.g., Ag, give rise to a larger contact area with good adhesion to next neighbors and show therefore an even lower contact resistance. Relatively soft materials however, tend to stick together and maintain a soldered-like connection. Even for large applied external forces it is hard to separate the particles [58,60].

In Table 2 resistivities of composites with similar filler volume fractions and particle sizes, but different filler hardness are listed. The soft Ag-coated Ni particles yield much lower resistance than the hard TiB_2 particles. Experiments by Ruschau et al. [49] show a similar trend. Additionally, they have developed a model taking into account not only elastic deformations according to Eq. 7 but also plastic deformations. They find good agreement with experimental data for Ag- and Ni-filled composites. For Cu and Al, however, the results were off by orders of magnitude. They assumed that surface oxide layers had a much stronger influence in these cases.

3.3. Filler Shape

In the previous sections, spherical particles were always assumed in modeling the composites. In

Table 2. Resistivities of composites with soft and hard fillers

Polymer	Filler	Filler content (vol. %)	Filler Vickers hardness (GPa)	Specific resistivity ($10^{-3}\,\Omega$ cm)
Spurr epoxy	Ni/Ag 10–15 μm	30	0.26[a]	6.0
HDPE	TiB_2, 10–30 μm	35	15–36[b]	56.2

[a]Values from [100].
[b]Values from [101].

practice, however, fillers are often used which have a shape very much different from a sphere. Examples are aluminum flakes, stainless steel fibers, carbon fibers or carbon black. As mentioned earlier, the percolation threshold can be drastically reduced for particles with an aspect ratio larger than one. This effect is illustrated in Fig. 5 for the statistical distribution of two-dimensional fillers on a two-dimensional plane [61]. The left picture shows a particle-like filler, the right picture a fiber-like filler with an aspect ratio of 200. The filler content is 10% of the area in both cases. By visual examination, one can easily observe connecting paths of the fibers. The particles, however, are isolated and no percolation can be observed. This illustrates that fillers with high aspect ratio can drastically reduce the percolation threshold.

Bigg et al. [62] studied experimentally, the influence of the aspect ratio for different kinds of carbon fibers. Figure 6 shows the relationship between aspect ratio and the minimum conductive filler concentration required to produce a composite having a volume resistivity below 100 Ω cm. Carbon fibers with an aspect ratio of 1000 need only 1 vol. %, whereas fibers with an aspect ratio of 10 need a volume fraction of about 10% in order to achieve the same resistivity. In the same study, the percolation of aluminum fibers and flakes with aspect ratios between 12.5 and 35 have been reported. Again the percolation threshold decreases with increasing aspect ratio.

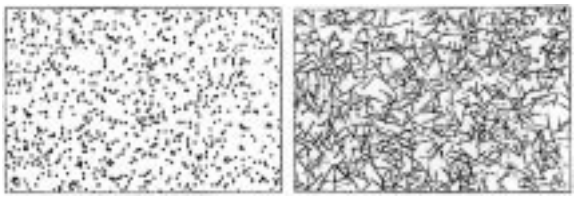

Fig. 5. Two-dimensional statistical distribution of powder-like particles (left) and fiber-like particles (right). The aspect ratio of the fibers is 200. The filler content is 10% of the area in both cases. Reprinted from [61].

The most common conducting filler is carbon black. For high conductivity it is produced either by thermal cracking of acetylene or by the synthesis gas process. The primary particles have sizes of only 10–100 nm. However, they agglomerate even during the production process to larger structures. Highly conducting carbon blacks exhibit a very large surface area, i.e., they are highly porous. The primary particles arrange in chains, which form a kind of tree structure. This provides a shift of the percolation threshold to low filler fractions, as sketched in Fig. 1 (dashed line). However, there are considerable differences between different types of carbon black [63].

In Fig. 7 the resistivities of composites containing fillers of different shape are compared: TiB_2 particles, Al fibers with aspect ratio 12.5, and conductive carbon black (Vulcan XC-72). The percolation threshold for

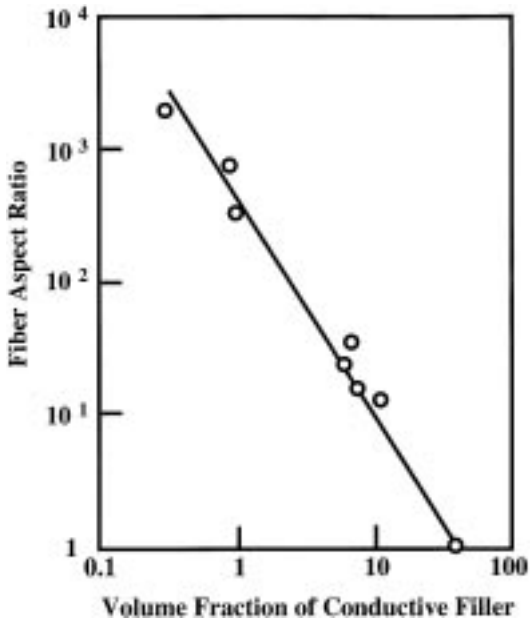

Fig. 6. Relationship between fiber-aspect ratio and minimum concentration required to produce a composite with a resistivity below 100 Ω cm [62].

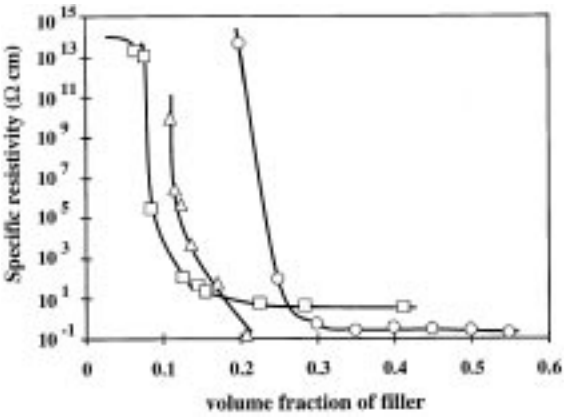

Fig. 7. Specific resistivity as a function of filler volume fraction for Vulcan XC-72 carbon black in rubber (□) [62], Al fibers with an aspect ratio of 12.5 (△) [62], and TiB_2 powder, sieved to 63–100 μm, in LDPE (○).

the TiB_2 particles is about 22%. The aluminum fibers percolate at 10–12% and the carbon black as low as 8%. Since carbon black is relatively cheap and only small amounts of powder are necessary to produce a conducting composite, it is widely used. Carbon black filled composites are utilized for anti-static transport boxes of electronic devices, anti-static chip carriers, toner material of copy machines and laser printers, the ground shield of cables and capacitive field control in high and medium voltage cable terminations. However, the lowest resistance, which can be achieved is limited to about 0.1–1 Ω cm. With metal fibers or metallic particles much lower resistivities are feasible, as can be seen from Fig. 7 as well. Aluminum flakes, or steel fibers are quite often used for EMI shielded housings of electronic equipment such as computers, monitors, cellular telephones or money teller machines.

3.4. Filler Distribution

The distribution of filler particles in a composite depends strongly on the chosen processing technique. For industrial production, extrusion or injection molding processes are used quite often. Using fibers, flakes or carbon black, the high shear forces occurring at the nozzle both methods cause an alignment of the filler particles in the flow direction. Hence, the orientation of the fibers or flakes in the final part depends strongly on the form of the mold and the flow of the polymer. An example of an injection molded heat sink containing aluminum flakes is shown in Fig. 8. Of course, the conductivity cannot be isotropic in such parts.

Care must be taken if composite parts are made by compression molding of polymeric and conductive powders. Figure 9 shows a cut through a press-sintered composite [61]. High-density polyethylene powder and carbon black were mixed and then compressed at elevated temperature. The carbon black particles are much smaller then the polymer particles. This results in a core-shell structure, which is clearly visible in Fig. 9. The polymer particles are surrounded by shells of carbon black, forming a percolating network. The percolation threshold of a core-shell structure is considerably lower than that of homogeneous composite. For the example of carbon black in polyethylene it is about 1% compared to 5–8% of homogenous distributed powder [64].

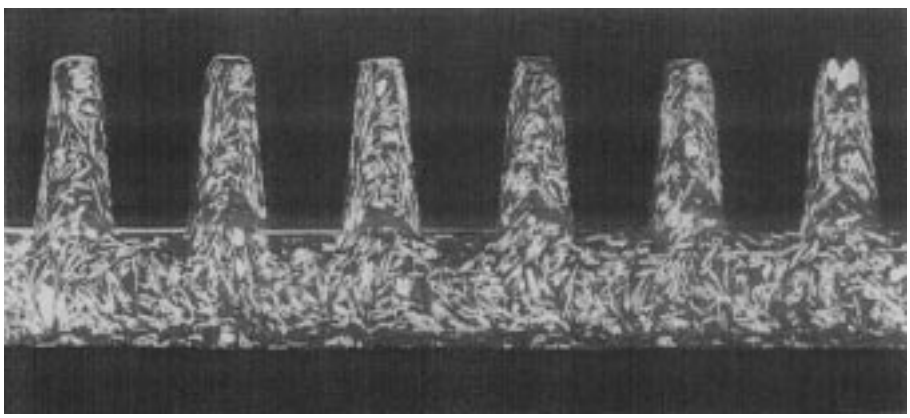

Fig. 8. Aluminum flakes in a molding compound for a heat sink. Courtesy of Transmet Corp., reprinted from [102].

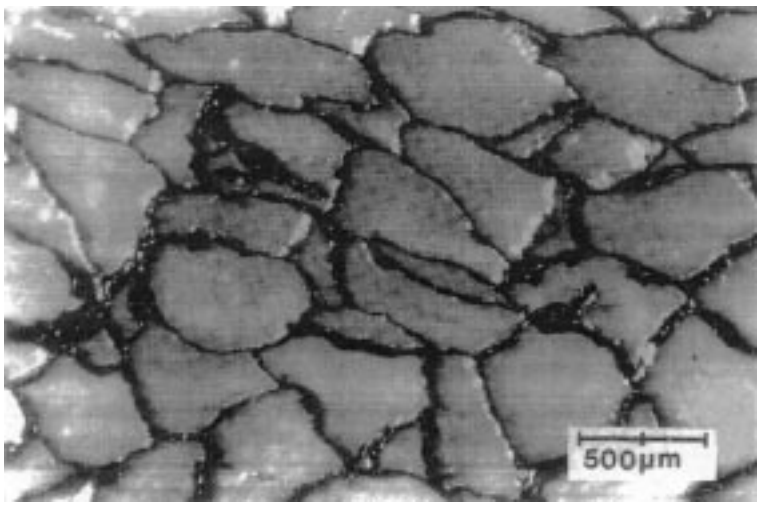

Fig. 9. Cut through a compressed plate made out of high-density polyethylene powder (Lupolen 5261 Z, Bayer AG) mixed with carbon black [61].

A controlled orientation of filler particles and an anisotropic conductivity can be achieved by applying electric or magnetic fields during the processing. This can serve not only for relative high conductivity at low filler content, but also for unidirectional conductivity. The orientation by electric fields has been studied mainly for dielectric purposes but no conductivity measurements have been published yet [65,66]. Various authors have already investigated the action of magnetic forces on conductor/polymer systems. Quite early, Gul and Golubera [67,68] reported on a composite system of metallic nickel powder in an epoxy matrix. They found incipient conductivities for < 1 vol. % and resistivities of 1–$10\,10^{-3}\Omega$ cm for 1–10 vol. % nickel content, if a dc magnetic field of 10^3–10^4 Am^{-1} was applied during hardening of the polymer matrix. This points to a string-like particle morphology in the composites. Agglomeration of the Ni particles in strands has been demonstrated also by a more recent, very special application of magnetic alignment [69,70]. Here, the purpose was to achieve an extreme degree of anisotropy, along with a very uniform particle dispersion in thin film composites. This has been achieved indeed with an anisotropy ratio larger than 10^{12} to 1. As a matrix polymer, a flexible silicone was chosen for applications of this special layer technology as interconnects in microelectronic packaging systems. For 20 μm nickel particles, a volume content of 5% was sufficient to achieve 25–70 mΩ in field direction at 25–30 μm thickness compared to 10^{10}–$10^{12}\,\Omega$ surface conductance perpendicular to the field. With long columns, such perfectly ordered composites have unidirectionally specific resistivities close to $10^{-3}\,\Omega$ cm for nickel fillers of about 75 μm average particle diameter and volume fractions of 5–10%.

3.5. Nonlinear Fillers

Very interesting and useful effects can be achieved by using nonlinear conducting fillers. Here, materials with a strong positive (PTC) or negative (NTC) coefficient of resistance, or varistor materials will be described. Well known PTC devices are made from ceramics such as $BaTiO_3$ or Cr-doped V_2O_3, which change their resistivity at the critical temperature by several orders of magnitude [71]. Attempts have been made to utilize the PTC effect of the filler for nonlinear properties of the composite [72]. The polymer matrix, however, quite often shows a stronger effect at similar temperatures.

Negative temperature coefficients of the resistance are well known as a common effect for all semiconducting materials. A very pronounced NTC effect around -125°C with a reversible change in resistivity by seven orders of magnitude is observed in V_2O_3. It is caused by a phase transition of the crystal structure and is the result of the formation of delocalized electrons [73]. Fine single crystal V_2O_3 particles dispersed in a polymer composite show the

same effect. Moffatt et al. [74] prepared polymer composites from a variety of different polymers, in which they dispersed up to 55 vol.-% single crystal V_2O_3 particles with a size of about 5 μm. Their data show an improved NTC effect for increasing filler content. A change in resistance of five orders in magnitude is observed for a flexible epoxy containing 50 vol. % V_2O_3.

The electrical conductivity of the filler may depend in a nonlinear way on the applied electrical field. Ceramic varistor (variable resistor) devices are made from doped ZnO. The ohmic $j(E)$ behavior at low voltage changes to a highly nonlinear relationship for electrical fields higher than the breakdown field E_B:

$$j \sim E^{\alpha} \tag{11}$$

For ceramic ZnO varistors the nonlinearity coefficient α is usually larger than 40 [75,76]. Polymer composites with a substantial varistor characteristic can be prepared by sintering spray-dried, doped ZnO varistor powder and mixing it into a polymer. The polycrystalline filler particles act as varistors due to their typical grain boundary structure. Such varistor composites containing 20 to 50 vol.-% of varistor filler can have nonlinearity coefficients α up to 30. Figure 10 shows a comparison of the $j(E)$ characteristic of an epoxy/varistor composite and a ceramic varistor material. The ceramic was sintered under the same conditions as the varistor filler. In the case of the composite, the leakage currents at low field are reduced by 1/8–1/3 and the breakdown field E_B is increased by a factor of about 1.5, compared to the bulk ceramic. The increase of E_B can be understood

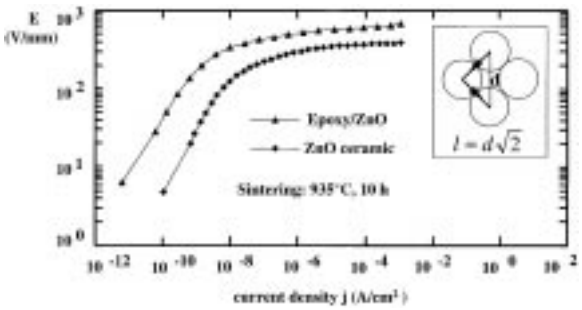

Fig. 10. $j(E)$ characteristics of a Spurr epoxy/43% varistor composite and a corresponding ceramic varistor. Powder and ceramic were sintered at 935°C for 10 h. Epoxy/ZnO: $E_B = 627$ V/mm (breakdown voltage at $j = 1.3 \cdot 10^{-4}$ A/cm^2), $\alpha_B = 32$ (nonlinearity coefficient at E_B), ZnO ceramic: $E_B = 379$ V/mm, $\alpha_B = 51$.

by the longer current path in the composite, while the reduced contact area explains the shift in the leakage current. For a dense packing of the powder in an FCC structure, the geometrical path length is increased by $\sqrt{2}$ (see insert of Fig. 10). In a close-packed HCP structure it would be a factor of $\sqrt{8/3} = 1.63$. This is close to the observed value. Together with the high α_B-values, it indicates that the varistor characteristic is dominated by the grain boundaries of the filler and not by the interfaces between the filler particles. Consequently, the characteristic can also be changed by the sintering conditions of the filler [77]. Using fillers with large grains, breakdown fields down to 200 V/mm can be achieved [78].

4. Influence of the Polymer Matrix on the Conductivity

The influence of mechanical and thermal properties of the polymer matrix on the electrical behavior of conducting composites requires further elucidation. Different materials like soft elastomers and rubbers, linear or branched thermoplastics or hard duromers as epoxies cover a wide range of mechanical properties.

As discussed before, the constriction resistance between filler particles depends on the forces between the grains. Higher contact forces may improve the conductivity. Hence, internal stresses in the polymer matrix caused by shrinkage, external mechanical actuation or thermal expansion play an important role for the conductivity of composites.

4.1. Internal Elastic Properties

A shrinkage of the polymer during processing can induce high internal stress. This reduces the interparticle resistance, but may also induce cracks and lead to failure during application. The origin of the shrinkage stress differs for duromers and elastomers on the one hand, and thermoplastics on the other. The curing and cross-linking of duromers and elastomers gives rise to a free volume reduction, which is responsible for the build-up of internal stresses. Thermoplastics are commonly processed above melting temperature and used for applications below this temperature limit. In this case, the thermal shrinkage during solidification creates the internal stress.

Miller [79] studied the resistivity of Ag-filler epoxy resins during curing. While the epoxy

hardened, the resistivity decreased by two to five orders of magnitude. Shear stress and resistivity were measured by Gul et al. [80] during the curing of nickel powder in epoxy. As the shear stress increased, the resistivity was reduced by five to seven orders of magnitude. A model for the calculation of the stress evolution in crosslinking polymers has been given by Adolf et al. [81].

An even larger change in resistance during curing is observed for TiB_2 fillers. Figure 11 shows the specific resistivity ρ and the internal temperature of an epoxy containing 46 vol. % TiB_2 during curing at 100°C. Surprisingly, the initial resistivity of $4 \times 10^6\,\Omega$ cm is quite high, although the filler particles have metallic conductivity and the filler fraction corresponds to the tap density. It seems that the contact pressure between the particles in the liquid epoxy is too low. During the first 30 min. the resistivity is reduced to $6 \times 10^4\,\Omega$ cm, while the temperature of the epoxy-powder mixture increases to 93°C. The reason may be an increasing conductivity of the epoxy resin with temperature, as measured for pure epoxy, also. But then, within the next 15 min., the resistivity increases again to a peak value of $2.5 \times 10^6\,\Omega$ cm. This may have two reasons. During gelation the resistivity of epoxy generally increases. Secondly, a separation of the particles can occur due to the expansion of the epoxy. In the succeeding 10 min. the resistivity is reduced by *eight orders of magnitude*. This is caused by a shrinkage of the epoxy, which increases the particle-particle pressure. The temperature increases in the meantime to a maximum of 106°C due the heat of reaction [82]. After a curing time of 75 min, ρ has stabilized at about $0.04\,\Omega$ cm and the temperature at 102°C. These values remain stable and unchanged until the completion of curing after 15 h. During the slow cool-down, a further reduction of the resistivity down to $0.01\,\Omega$ cm is caused by the thermal contraction of the composite.

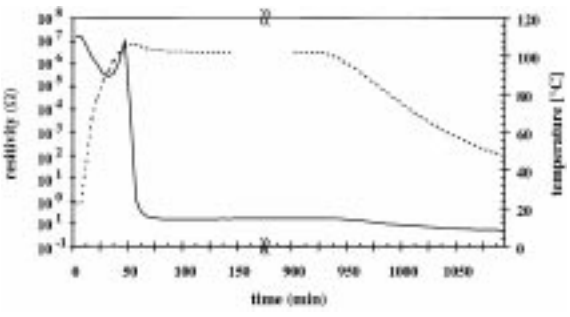

Fig. 11. Spurr B epoxy/46 vol. % TiB_2 during curing at 100°C: specific resistivity (plain line) and temperature (dashed line).

This example shows that the thermal contraction of a composite can have a huge influence on the electrical resistivity. Since a filler fraction of 46% is far beyond the percolation threshold for particles, this effect cannot be explained in terms of percolation theory. Instead, the observed strong resistivity change is caused by a release of particle-particle contact pressure and a change in gap distance. It should be noted that the resistivity change during curing is the smallest for Ag, medium for Ni and highest for TiB_2. This reveals again the influence of the filler hardness (section 3.2). Due to the hardness of TiB_2, the particles do not stick together and make the resistivity of the composite sensitive to small micro-mechanical changes. In addition the influence the particle size shall be mentioned again. If the particle size is reduced, the internal stress generated during processing is distributed to a larger number of contacts. That means a reduction of the contact forces and a further increase of the resistance according to Eq. 7.

4.2. External Mechanical Actuation

Similar changes in resistivity can be achieved if stress is applied externally. This can lead to a change in conductivity through a change in the distribution of the filler particles, especially at low filler contents in soft polymers, due to their low Young's Moduli. At higher filler content, i.e., for more rigid composites, it is more likely to modify the number and efficiency of the electrical contacts by the application of external forces. This effect has been demonstrated by Carmona et al. [83] for flexible composites filled with carbon black and graphite fibers. The initial resistivity of about $10^3\,\Omega$ cm is reduced by a factor of two under an applied hydrostatic or uniaxial pressure of 100 MPa and 1.5 MPa for Araldite epoxy and Rhodorsil silicone, respectively. Larger resistivity changes have been observed by Yoshikawa et al. [84] using Fe_3O_4 or SnO_2 in a flexible epoxy matrix. Under an uniaxial pressure of 20 MPa the resistivity of a composite containing 22% SnO_2:Sb (particle size $< 0.1\,\mu$m) is reduced from about 10^8 down to $10^6\,\Omega$ cm. In the case of Fe_3O_4 (particle size: $0.2\,\mu$m), the maximum reduction is observed for a filler content of 47 vol. %. The resistivity of $10^6\,\Omega$ cm is reduced down to $10^3\,\Omega$ cm by an applied pressure of 10–12 MPa.

Larger resistivity changes can be achieved by using a hard oxide-free filler material as in section 4.1. Figure 12 shows the resistivity as a function of uniaxial pressure for different filler contents of TiB_2 (particle size: 100–200 μm) in Powersil 250 Q silicone rubber. The composite was compounded using a Brabender plasticorder at 60°C. The mixture was then pressed to form a plate of 4–6 mm thickness and vulcanized at 180°C for 20 min. For the highest and lowest filler content, the pressure dependence under an uniaxial pressure of 10 MPa is relative small (three orders of magnitude). Between 25 and 35 vol. %, however, the resistivities change by six to eight orders of magnitude. This means that for intermediate filler contents not only the particle-particle contact is improved by an applied pressure, but also additional conducting paths are established.

In a similar way, extensional strain can change the resistivity, as reported for nitrile-rubber filled with carbon fibers. The specific resistivities of the initial state were between 0.3 and 2 Ω cm. A strain of 40% resulted in a reduction of ρ by a factor of 8 to 10 [85].

4.3. Thermal Properties

Polymers can show three significant reversible structural transitions, which are thermally induced: crystallization and melting in a semi-crystalline phase and a glass transition in the amorphous phase. All three transitions are related to a relative large volume change or to a pronounced change in the thermal expansion (Table 3). The thermal expansion of the polymer matrix exerts a considerable influence on the electrical conductivity.

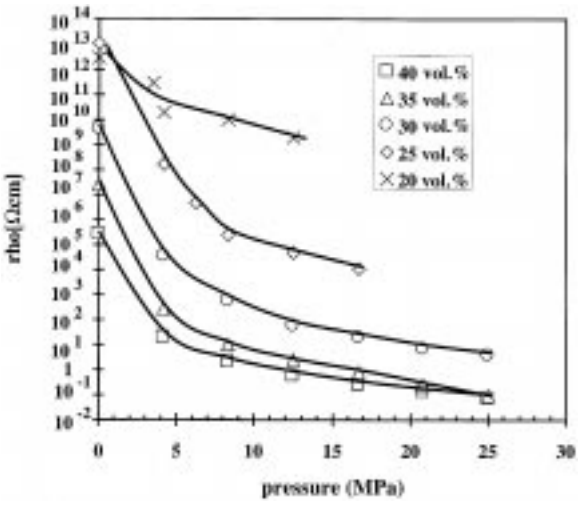

Fig. 12. Resistivity as a function of uniaxial pressure for 25, 30, 35 and 40 vol. % of TiB_2 in silicone rubber (Powersil 250 Q).

A strong positive temperature coefficient (PTC) of resistance in conducting polymers close to the melting temperature was first discovered by Pearson at Bell Labs in 1939 [86], then studied by Frydman [87] in 1945, forgotten for a while, and rediscovered by Kohler [88] in 1961. Unlike Frydman, Kohler observed a significant resistivity change of about one order of magnitude and industrial interest was immediately aroused. Since the work of Kohler much attention has been paid to polymeric PTC materials [74, 89–93].

Figure 13 shows the temperature dependence of the heat flow in differential scanning calorimetry (DSC), and the resistivity and relative linear expansion as measured by dilatometry for a 50 vol. % TiB_2 / HDPE composite [94]. The composite material has an initial temperature resistivity of about 0.01 Ω cm. Far below the melting temperature the resistivity increases only gradually with increasing temperature. But upon approaching the melting temperature of the matrix, which is determined by DSC as 133°C (Fig. 13a), a huge step-like increase of more than eight orders of magnitude is observed (Fig. 13b). Also the thermal expansion (Fig. 13c) exhibits a stronger increase in the same temperature range.

Well below the melting temperature of the polymer, the conducting filler particles are in a state of close packing with intimate contact to next neighbors, forming conducting paths throughout the composite. During heating, the polymer expands much more then the filler particles themselves. The contact pressure between adjacent filler particles is reduced leading to a moderate resistivity increase for $T < 120$°C, as shown in Fig. 13b. The effect is strongly enhanced when approaching the melting temperature of the polymer matrix. There the filler particles and the conducting paths are obviously interrupted due to the enhanced thermal expansion of the polymer. This

Table 3. Properties of phase transitions in polymers

Transition	Important property of interest
Crystallization	Shrinkage, densification
Melting	Expansion
Glass transition	Freezing, introduction or release of internal stress

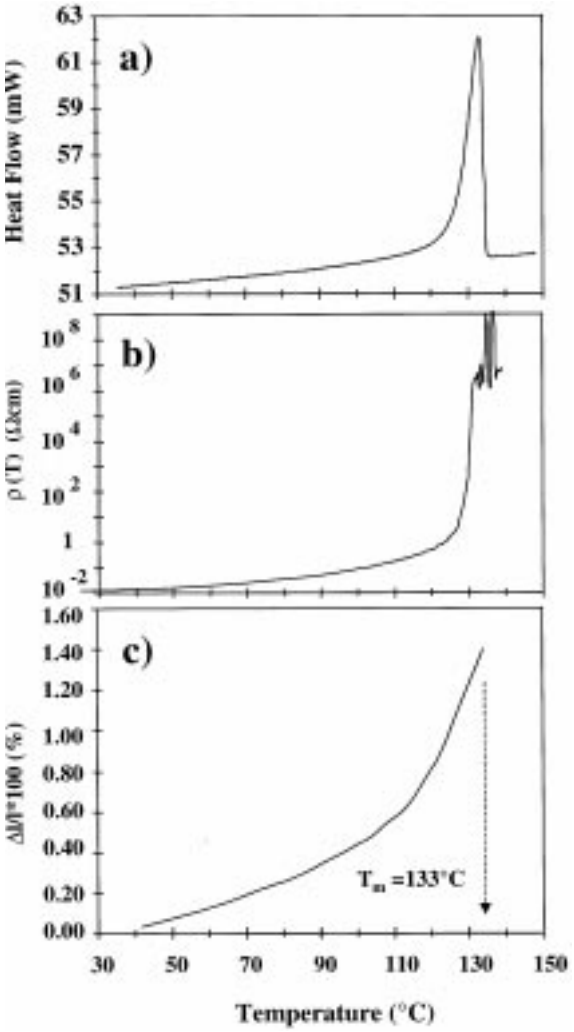

Fig. 13. Results of the heat flow in DSC (top), the resistivity (middle) and the relative linear expansion (bottom) of 50 vol. % TiB_2 in HDPE are shown as a function of temperature.

leads to the huge jump in the resistivity. This view is supported by similar results for carbon black dispersed in polyethylene [95].

The transition from low resistivity to high resistivity can be utilized for current limitation. Such limiters are presently available as small elements for the protection of circuit boards at rated currents between fractions of an Ampère to several Ampères [5]. As a three-phase current limiting module [9], they are used in low voltage distribution systems for ratings up to 63 A. Even for very fast current limitation, it could be shown by optical methods that the origin for the resistivity increase is the expansion of the composite material [96,97].

Most of the resistance of the PTC material in the conducting state originates from constriction resistance at the contact points. Therefore, the contact points are the dominant sources of heat in the material. The thermal conductivity of most of the conducting filler materials ($1–10^2$ W/Km) is at least one order of magnitude higher than that of the polymer matrix (< 0.3 W/Km). Consequently, one can show from the heat equation that the generated heat dissipates first, within 1–10 μs, into the filler particles [50]. Then, with a time delay of 0.2–0.5 ms, the matrix is heated as well. Therefore the temperature distribution inside the filler particle will be quite homogenous, except in the close vicinity of the contact spots, where temperatures up to 3000 K can be expected [46].

Experiments on metal-filled composites with variable filler particle sizes from 1 to 200 μm show a strong correlation between particle size and heating of the composite material by Joule losses at the contact spots. The samples were exposed to high power current pulses using a low impedance test set-up. The development of the resistivity of the samples was monitored on a microsecond time scale. It was demonstrated that the best current limitation occurs for composites containing the smallest particles [50]. The reason is that the location of heat generation is much more uniform in a composite containing small particles. Hence, within a certain period of time a larger part of the polymer can be heated to the critical temperature. It has been shown that within only 150 μs the composite starts to limit and current densities of about 10 kA/cm^2 can be switched off within 200 μs.

4.4. Stability and Endurance

In addition to the long-term properties of polymers and polymer composites, as they are known in general, conducting composites are very sensitive to changes in the inter-particle resistance due to environmental influences. If the composite is operated or aged at elevated temperature, metallic filler materials can easily oxidize, drastically reducing the conductance [98]. Also for carbon blacks a strong resistivity increase has been observed by Meyer [99] in the presence of oxygen at elevated temperature. In addition, the mechanical properties of the polymer are changed upon continuous heating. Meyer reported

that the total expansion of polyethylene/carbon black is considerably reduced after aging at 150°C for 39 days. During the same time the degree of crystallinity is reduced by about 50%. As a considerable part of the expansion is due to melting of crystalline areas, this must consequently have a strong influence on the PTC anomaly. Therefore, it is not surprising that Meyer also found a reduction of the resistivity ratio $\log(\rho_{\max}/\rho_{25°C})$ of the PTC effect from 4 to about 0.2.

Active heating of the composite by a current can lead to similar aging phenomena. In particular for high power applications this is especially important since it can change the operational characteristics of a device. For PTC devices it is known that the resistance increases by at least 20% after the first fast self-heating by a current [5]. The recovery of the resistance to its initial value takes place very slowly during several days. The origin of this process probably involves secondary recrystallization of the polymer and reorganization of the filler chains.

Most polymers used for conducting composites show decomposition when they are exposed to temperatures above 300°C. Consequently, heating by over-currents to such temperatures can lead to irreversible changes of the polymer which alter the mechanical and electrical properties of the composite.

5. Conclusions

In this paper we have given an overview on the major physical properties of the polymer and the filler which determine the conductivity of polymer composites. It turns out that many characteristics of the filler as well as of the matrix have a strong influence. This is of particular importance for practical use, since quite often a combination of desired properties is not possible. The shape of the filler, for example, depends on the material structure and the processes, which are available to prepare the selected material in the form of particles, flakes or fibers. Especially commercial filler materials are limited very much in this respect. Moreover the importance of composite processing is quite often underestimated. As an example we have shown how large the difference can be between compounding and press-sintering. Although it is difficult to predict quantitatively the difference in conductance, it is important for applications to be aware of the trend. From the theoretical point of view, the described models provide at least indications of functional dependencies. However, a general model, which includes the electrical contact between particles, the particle deformation and the mechanical properties of the polymeric matrix is still missing and would be of great practical value.

Acknowledgment

The authors wish to thank Felix Greuter, Jørgen Skindhøj, Jan Isberg and Claus Schüler for many helpful discussions, and Ruzica Loitzl, Andreas Garbin and Markus Zehnder for experimental support.

References

1. R.P. Kusy, in *Metal-Filled Polymers,* edited by S.K. Battacharya (Dekker, New York, 1986) p. 1.
2. D. Luch, U.S. Patent 4,009,093 (Feb. 22, 1977)
3. D.M. Lindsey, *Prod. Finish* July 1979, 34–43 (1979).
4. F. Bueche, *J. Appl. Phys.*, **44**, 532 (1973).
5. F.A. Doljack, *IEEE Trans. on Comp., Hybrids and Manufact. Techn. CHMT-4*, 372 (1981).
6. T. Fang, St Morris, *Elektron*, January 97, 103–104 (1997).
7. M. Stoessl, *Power Control in Motion*, June 93, 50–55 (1993).
8. T. Kobayashi and H. Endo, *NEC Research and Development*, **86**, 81–90 (1987).
9. T. Hansson, *ABB Review*, **4/92**, 35 (1992).
10. R.H. Norman, *Conductive Rubbers and Plastics* (Applied Science Publishers, London, 1970).
11. *Carbon Black—Polymer Composites*, edited by E.K. Sichel (Dekker, New York, 1982).
12. J. Delmonte, *Metal/Polymer Composites* (Van Nostrand Reinhold, New York, 1982).
13. L.K.H. van Beek, *Progr. Dielect.*, **7**, 69 (1967).
14. S. Nakamura, A. Ito, G. Sawa, and K. Kitagawa, *Electronics and Communications in Jpn. 2, Electron. (USA)*, **75**(3), 109 (1992).
15. K.T. Chung, *Org. Coat. Appl. Polym. Sci. Proc.*, **48**, 661 (1983).
16. P. Hedvig, *Dielectric Spectroscopy in Polymers* (Wiley, New York, 1977).
17. E.K. Sichel, J.I. Gittleman, and P. Sheng, *Phys. Rev. B*, **18**, 5712–16 (1978).
18. A.I. Medalia, *Rubber Chemistry and Technology*, **59**, 432–454 (1986).
19. P. Sheng, *Phys. Rev. B*, **21**, 2180–95 (1980).
20. R.D. Sherman, L.M. Middleman, and S.M. Jakobs, *Polym. Eng. and Sci.*, **23**, 36–46 (1983).
21. I. Balberg, *Phys. Rev. Let.*, **59**, 1305–08 (1987).
22. D.S. McLachlan, M. Blaszkiewicz, and R.E. Newnham, *J. Am. Ceram. Soc.*, **73**, 2187–2203 (1990).
23. R.E. Newnham, D.P. Skinner, and L.E. Cross, *Mat. Res. Bull.*, **13**, 525 (1978).

24. R. Zallen, *The physics of amorphous solids* (Wiley, New York, 198) ch. 4.
25. D. Staufer, *Introduction to percolation theory* (Taylor and Francis, London, U.K., 1985).
26. S. Kirkpatrick *Rev. Mod. Phys.*, **45**(4), 574 (1973).
27. W.Y. Hsu, W.G. Holtjeand, and J.R. Barkley, *J. Mat Sci. Lett.*, **7**, 459 (1988).
28. J.P. Straley, in Vol. 5, *Annals of the Israel Physical Society: Percolation Processes and Structures*, edited by G. Deutscher, R. Zallen, and J. Adler (Israel Physical Society, Jerusalem, 1983), p. 353.
29. G.R. Ruschau, S. Yoshikawa, and R.E. Newnham, *Proceedings of the 42th Electr. Components & Technology Conf.* San Diego, CA, May 18–20, p. 481 (1992).
30. R. Landauer, in *American Institute of Physics Conference Proceedings: Electrical Transport and Optical Properties of Inhomogeneous Media,* edited by J.C. Garland and D.B. Tanner (American Institute of Physics, New York, 1978), No. 40, p. 2.
31. D.S. McLachlan, *J. Phys.*, **C21**, 1521 (1988).
32. D.S. McLachlan, *Mat. Res. Soc. Symp. Proc.*, **411**, 309 (1996).
33. K.C. Kao and W. Hwang, *Electrical Transport in Solids, Int. Series in the Science of the Solid State*, Volume 14 (Pergamon Press, Oxford, 1981).
34. A.R. Blythe, *Electrical properties of polymers* (Cambridge University Press, Cambridge, 1979).
35. L.K.H. van Beek et al., *J. Appl. Polymer Sci.*, **6**(24), 651 (1962).
36. J. Frenkel, *Physical Review*, **36**, 1604 (1930).
37. W. Imaino, K. Loeffler, and R. Balanson, in *Colloids and Surface in Reprographic Technology ACS Symposium Series 200*, p. 249 (American Chemical Society, Washington, 1982).
38. R. Holm, *Electrical Contacts, Theory and Application* (Springer, New York, 1967).
39. G.R. Ruschau, S. Yoshikawa, and R.E. Newnham, *J. Appl. Phys.*, **81**(10), 6786 (1997).
40. A.W. Bush, Contact Mechanics, in *Rough Surfaces* edited by T.R. Thomas et al. (Longman, London, 1982).
41. Y.A. Dzenis and V.M. Ponomarev, *Mek. Komp. Mat.*, **1**, 70 (1988).
42. R. Shima et al., *Polymer Composites*, **10**(6), 409 (1989).
43. T.T. Wang and T.K. Kwei, *J. Polym. Sci.: Polym. Phys.*, **7**(5), 889 (1969).
44. B. Budiansky, *J. Comp. Mat.*, **4**, 284 (1970).
45. N.W. Ashcroft and N.D. Mermin, *Solid State Physics* (Holt, Rinehart & Winston, Philadelphia, 1976).
46. M. Heuberger, G. Dietler, R. Strümpler, J. Rhyner, and J. Isberg, *J. Appl. Phys.*, **82**(3), 1255 (1997).
47. K. Ohe and Naito, *Jap. J. Appl. Phys.*, **10**(1), 99 (1971).
48. A.D. McLeod, J.S. Haggerty, and D.R. Sadoway, *J. Am. Ceram. Soc.*, **67**, 705 (1984).
49. G.R. Ruschau, S. Yoshikawa, and R.E. Newnham, *J. Appl. Phys.*, **72**, 953 (1992).
50. R. Strümpler, G. Maidorn, and J. Rhyner, *J. Appl. Phys.*, **81**(310), 6786 (1997).
51. J.I. Pascual, J. Méndez, J. Gómez-Herrero, A.M. Baró, N. Garcia, U. Landman, W.D. Luedtke, E.N. Bogachek, and H.-P. Cheng, *Science*, **267**, 1793 (1995).
52. L. Zimmermann, M. Weibel, W. Caseri, and U.W. Suter, *Polym. for Adv. Techn.*, **4**, 1–7 (1992).
53. J.P. Spatz, A. Roescher, and M. Möller, *Adv. Mater.*, **8**(4), 337 (1996).
54. M.P.J. van Staveren, H.B. Brom, and L.J. de Jongh, *Physics Reports*, **208**, 1–96 (1991).
55. G. Schön and U. Simon, *Colloid Polym. Sci.*, **273**, 101–117 (1995).
56. A. Tampieri and A. Bellosi, *J. Mat. Sci.*, **28**, 649 (1993).
57. *The Oxide Handbook*, edited by G.V. Samsonov (Plenum Press, New York, 1981).
58. R. Strümpler, *J. Appl. Phys.*, **80**(11), 6091 (1996).
59. R. Strümpler, R. Loitzl, and L. Ritzer, European Patent 0 696 036 A1 (July 12, 1995).
60. S. Littlewood and B.F.N. Briggs, *J. Phys. D: Appl. Phys.*, **11**, 1457–62 (1978).
61. K.-H. Möbius in *Elektrisch leitende Kunststoffe*, edited by H.J. Mair and S. Roth (Carl Hanser, Munich, 1989) p. 59.
62. D.M. Bigg and D.E. Stutz, *Polym. Comp.*, **4**, 40 (1983).
63. W.F. Verhelst, K.G. Wolthuis, A. Voet, P. Ehrburger, and J.B. Donnet, *Rubber Chem. and Techn.*, **50**, 735–46 (1977).
64. R.G. Gilg in *Elektrisch leitende Kunststoffe,* edited by H.J. Mair and S. Roth (Carl Hanser Verlag, München, 1989), p. 21.
65. C.A. Randall, D.V. Miller, J.H. Adair, and A.S. Bhalla, *J. Mater. Res.*, **8**, 899 (1993).
66. Y.-S. Ho and P. Schoen, *J. Mater. Res.*, **11**, 469 (1996).
67. V.E. Gul and M.G. Golubeva, *Koll. Zh.*, **28**, 62 (1967).
68. V.E. Gul and M.G. Golubeva, *Koll. Zh.*, **30**, 13 (1968).
69. S. Jin, R.C. Sherwood, J.J. Mottine, T.H. Tiefel, R.L. Opila, and J.A. Fulton, *J. Appl. Phys.*, **64**, 6008 (1980).
70. S. Jin, T.H. Tiefel, L.-H. Chen, and D.W. Dahringer, *IEEE Trans. on Components, Hybrids, and Manufact. Techn.*, **CHMT-16**, 972 (1993).
71. R.S. Perkins, A. Rüegg, M. Fischer, P. Streit, and A. Menth, *IEEE Trans. on Components, Hybrids, and Manufact. Techn*, **CHMT-5** (2) (1982).
72. F. Greuter and R. Strümpler, European Patent 0 649 150 B1 (1994).
73. J. Feinleib and W. Paul, *Phys. Rev.*, **155**, 841 (1967).
74. D.M. Moffatt, J.P. Runt, A. Halliyal, and R.E. Newnham, *J. Mat. Sci.*, **24**, 609 (1989).
75. J. Pedulla and P. Malinaric *in EOS/EOD Symp. Proc.*, (1981) 49–56.
76. *Adv. in Varistor Tech., Ceramic Transactions 3*, edited by L.M. Levinson (1989).
77. R. Strümpler, P. Kluge-Weiss, and F. Greuter, *Adv. Sci. Technology 10, Int. Mat. and Syst.*, edited by P. Vincenzini (Techna S.r.I., Faenza, Italy, 1995) p. 15.
78. J. Glatz-Reichenbach, B. Meyer, R. Strümpler, P. Kluge-Weiss, and F. Greuter, *J. Mat. Sci.*, **31**, 5941 (1996).
79. B. Miller, *J. Appl. Polymer Sci.*, **10**, 217–228 (1966).
80. V.E. Gul, L.Z. Shenfil, and G.K. Melnikova, *Soviet Plastics*, **3**, 68–70 (1960).
81. D. Adolf and J.E. Martin, *J. of Composite Materials*, **30**(1), 13 (1996).
82. R. Strümpler, G. Maidorn, A. Garbin, and F. Greuter, *Polymers and Polymer Composites*, **4**, 299–304 (1996).
83. F. Carmona, R. Canet, and P. Delhaes, *J. Appl. Phys.*, **61**, 2550 (1987).
84. S. Yoshikawa, T. Ota, and R. Newnham, *J. Am. Ceram. Soc.*, **73**, 263–267 (1990).

85. P.K. Pramanik, D. Khastagir, and T.N. Saha, *J. Mat. Sci*., **28**, 3539–3546 (1993).
86. G. Pearson, US Patent 2,258,958 (Oct. 14, 1941).
87. E. Frydman, UK Patent Spec. 604 695 I 718 14S (July 8, 1948).
88. F. Kohler, US Patent 3,243,753 I 3/29/66 (Mar. 29, 1966).
89. K. Ohe and Y. Natio, *Jap. J. Appl. Phys*., **10**, 99–108 (1971).
90. J. Meyer, *Polymer Eng. and Sci*., **13**, 462–468 (1973).
91. A. Voet, *Rubber Chemistry and Technology*, **54**, 42–50 (1980).
92. K.A. Hu, J. Runt, A. Safari, and R.E. Newnham, *Phase Transitions*, **7**, 1–4 (1986).
93. T.R. Shrout, D. Moffatt, and W. Huebner, *J. Mat. Sci*., **26**, 145–154 (1991).
94. J. Glatz-Reichenbach, F. Greuter, J. Skindhøj, and R. Strümpler, *Proc. of 5th Int. Conf. on Comp. Eng*. (ICCE/5), July 5–11, 1998, edited by D. Hui, p. 321 (1998).
95. M.B. Heaney, *Appl. Phys. Lett*., **69**, 2602 (1996).
96. J. Skindhøj, J. Glatz-Reichenbach, and R. Strümpler, *IEEE Trans. PWRD*, **13**, 489–94 (1998).
97. J. Glatz-Reichenbach, J. Skindhøj, and R. Strümpler, *Proc. of 11th Int. Conf. on Comp. Mater.,* vol. 5 (ICCM-11), Gold Coast, Australia, July 14–18, 1997, edited by M.L. Scott (Woodhead Publ., 1997) pp. 749–758.
98. V.E. Gul, L.Z. Shenfil, G.K. Melnikova, and A.S. Poluden, *Soviet Plastics*, **7**, 60–62 (1966).
99. J. Meyer, *Polymer Eng. and Sci*., **14**, 706 (1974).
100. H. Wagar, in *Physical Design of Electronic Systems*, vol. 3 (Prentice Hall, Englewood Cliffs, N.J., 1971).
101. W.J. Lackey, D.P. Stinton, G.A. Cerny, A.C. Schaffhauser, and L.L. Fehrenbacher, *Adv. Ceram. Mat*., **2**, 24–30 (1987).
102. J. Delmonte, *Metal / Polymer Composites* (Van Nostrand, New York, 1998) p. 173.